Comparative study of electroabsorption spectra of polar and nonpolar organic molecules in solution and in a polymer film

Comparative study of electroabsorption spectra of polar and nonpolar organic molecules in solution and in a polymer film

Jumpei Tayama, Toshifumi Iimori, and Nobuhiro Ohta[a)]
Research Institute for Electronic Science, Hokkaido University, Sapporo 001-0020, Japan

(Received 4 August 2009; accepted 23 November 2009; published online 29 December 2009)

Electroabsorption (EA) spectra of polar and nonpolar molecules of coumarin 153 (C153) and pyrene in solution and in a polymer film of polymethylmethacrylate (PMMA) have been measured in the UV-visible region at room temperature. The shape of the EA spectra of C153 in benzene, 1,4-dioxane, or monochlorobenzene remarkably depends on the angle between the polarization direction of the absorption light and the applied electric field, whereas the EA spectra of C153 doped in PMMA show only the Stark shift and the field-induced change in spectral shape is negligible. These results demonstrate that C153 is reoriented by application of electric fields in solution, but the molecules are immobilized in a PMMA film. Based on the EA spectra, electric dipole moments both in the ground state and in the excited state have been evaluated for C153 in different solvents. In the EA spectra of pyrene, only the Stark shift is observed both in solution and in PMMA, indicating that the field-induced molecular reorientation does not occur both in solution and in PMMA. The change in dipole moment of C153 as well as the change in molecular polarizability of pyrene following absorption is much larger in solution than that in PMMA. © *2009 American Institute of Physics*. [doi:10.1063/1.3273875]

I. INTRODUCTION

Manipulation of the molecular orientation has been extensively pursued in modern science. Polar molecules can be spatially oriented by using strong electric fields and the rotational motion changes to a pendulumlike libration, that is, pendular states, if the interaction energy between electric fields and the electric dipole moment of molecules exceeds the rotational energy in the gas phase.[1,2] In solutions, the alignment induced by strong electric fields leads to electric dichroism, and the birefringence caused by the field-induced alignment is known as the Kerr effect.[3] However, manipulation as well as detection of the molecular reorientation in solution is not so easy for small molecules since the degree of orientation is rather small with field strengths at which the dielectric breakdown does not take place.

Electroabsorption (EA) spectroscopy, in which electric field-induced change in absorption spectrum is measured, is a powerful technique to investigate the molecular reorientation induced by external electric fields.[4] When probed molecules are embedded in the solid matrix such as molecular crystals, polymers, or organic solvent glasses, embedded molecules are usually immobilized in the matrix,[5–10] except for some molecules in a polymer film which somehow exhibit the field-induced orientation effect.[11,12] In solution, on the other hand, molecules are easily reoriented and the field-induced reorientation can be detected by the EA measurements.[13–15] However, the precise measurements of the EA spectra in solution are not so easy due to the difficulty in application of strong electric fields to solutions.

Not only for the study of molecular reorientation but also for the study of electronic structure in the excited states, the measurements of external electric field effects on optical absorption spectra and on emission spectra are extremely useful.[4–13,16] One of the central issues in physical chemistry is certainly the understanding of the electronic structure in the ground state as well as in the electronic excited states of molecules, and electric dipole moment ($\boldsymbol{\mu}$) and molecular polarizability ($\boldsymbol{\alpha}$) in each state give a significant information about the electronic structure. One of the classical approaches to the evaluation of $\Delta\boldsymbol{\mu}$ has been the analysis of the solvent-dependent spectral shifts. The magnitude of the difference between the absorption energy and fluorescence energy, that is, the Stokes shift, is related to the $\Delta\boldsymbol{\mu}$ of the fluorescent molecule according to the Lippert–Mataga equation.[17,18] This method has been successfully applied to many molecules so far in solution to estimate $|\Delta\boldsymbol{\mu}|$. In this method, however, emission measurements are necessary, and the information about the molecular polarizability cannot be obtained. On the other hand, not only $|\Delta\boldsymbol{\mu}|$ but also $\Delta\boldsymbol{\alpha}$ may be able to be evaluated from the EA spectra.

In the present study, we have constructed a liquid cell which enables us to measure easily and precisely EA spectra of solution samples in the UV-visible region. EA spectra of two frequently used probe molecules, i.e., coumarin 153 (C153) and pyrene have been measured in solution as a representative of polar and nonpolar molecules, respectively. C153 has a large dipole moment, while pyrene is a nonpolar molecule which belongs to D_{2h} point symmetry group in the ground state. EA spectra of these two compounds doped in a polymethylmethacrylate (PMMA) solid film have been also measured for the direct comparison between EA spectra in

a)Author to whom correspondence should be addressed. Electronic mail: nohta@es.hokudai.ac.jp.

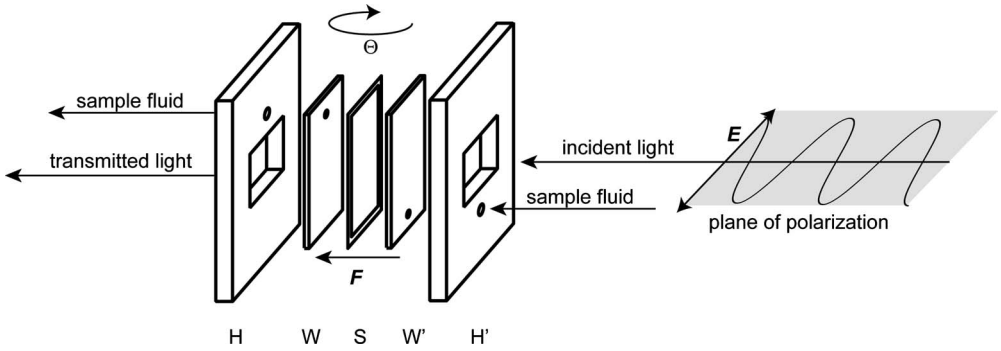

FIG. 1. The design of the used liquid cell. (H,H′) The cell holder: (W,W′) quartz plates on which ITO and silicon oxide films are coated; (S) a polymer film spacer. ***E*** is the polarization direction of the incident light. ***F*** is the direction of the applied electric field. Θ is the rotation angle of the cell with which the angle between ***E*** and ***F*** is changed.

solution and in solid matrix, though EA spectra of these compounds in polymer matrices and organic glasses were already reported.[19,20]

II. EXPERIMENTAL

C153 (Lambda Physik), benzene (Kanto Chemical, spectroscopy grade), and 1,4-dioxane (Wako Pure Chemical, infinity pure grade) were used without further purification. Monochlorobenzene (Wako Pure Chemical, spectroscopy grade) was used following the further purification by distillation. Pyrene (Aldrich) was purified by recrystallization. The concentration of the solution was $(1-3)\times 10^{-2}$ mol/dm^3. Polymer films of C153- or pyrene-doped PMMA were also prepared with the same method as reported elsewhere.[20,21] Briefly, PMMA (Aldrich, averaged MW=120 000) was purified by a precipitation with a mixture of benzene and methanol and by extraction with hot methanol. A benzene solution of PMMA and C153 or pyrene was cast on a quartz substrate that was coated with indium tin oxide (ITO) and the thin film was obtained using a spin coating technique. A semitransparent aluminum (Al) film was deposited on the dried polymer film. The ITO and Al films were used as electrodes. The thickness of the PMMA layer was measured using an interferometric microscope system (Nanometrics, M3000). The concentration of the sample, which was calculated as the molar ratio to the monomer unit of PMMA, was 1 mol % for both C153 and pyrene.

For the measurements of the EA spectra in solution, the liquid cell was consisted of two ITO-coated quartz windows, which used semitransparent electrodes, as shown in Fig. 1. A silicon-oxide film was evaporated on the ITO-film as an insulator film with a thickness of 0.2–0.4 μm. Between the electrode surfaces, a Mylar film spacer with 6 μm was placed to create a gap having a specific distance. The actual distance of the electrode gap after assembling the liquid cell was evaluated from the optical interference fringe in the transmitted light intensity. The field strength was evaluated from the voltage applied to the cell divided by the gap distance. By using the newly constructed liquid cells, the maximum field strength that we could apply to the cell was as strong as 0.2 MV cm^{-1}. As occasion demands, the sample solution was circulated through the gap between the electrodes using a peristaltic pump.

EA spectra were measured using a spectrometer (Jasco, EMV-100), which covers wavelengths from UV to near-infrared region. The light beam from a xenon lamp was monochromated, linearly polarized with a UV polarizer, and directed through the sample to a photomultiplier tube. The measurements were performed with a slit-width of 5 nm. The signal from the photomultiplier tube was amplified and directed both to a dual-phase digital lock-in amplifier (Stanford Research System, SR830) and to an analog-to-digital converter. The modulation in absorption intensity was induced by application of a sinusoidal ac voltage having a frequency of 1.5 or 2 kHz to the sample. Field-induced change in the transmitted light intensity ($\Delta I(2\omega)$) was detected at the second harmonic (2ω) of the frequency of the applied voltage by using the lock-in amplifier. The dc component of the transmitted light intensity (I) was recorded using the analog-to-digital converter. The field-induced change in absorption intensity, that is, the EA spectrum, was obtained as

$$\Delta A = -(2\sqrt{2}/\ln 10)\Delta I(2\omega)/I, \tag{1}$$

where the factor $2\sqrt{2}$ converts the value of the measured rms $\Delta I(2\omega)$ signal to its value as if measured with a static electric field, and the factor 1/ln 10 comes from the expansion of the formula of the absorbance $A=-\log(I/I_0)$ on the assumption of the small change in I.

The EA spectra were measured at different angles χ between the polarization direction (***E***) of the absorption light and the direction of the electric field (***F***) applied to the sample. To change the angle χ, we changed the incident angle θ of the p-polarized absorption light. The angles θ and χ obey Snell's law of refraction[12]

$$\cos\theta = n\cos\chi, \tag{2}$$

where n is a refractive index of the sample and the refractive index of the air was approximately taken as 1. The value of n for the solvents used in the present work was assumed to be equal to its n_D value at room temperature.[22] From Eq. (2), we determined the value of χ. All the measurements were performed in ambient air at room temperature. The applied field strength $F=|\boldsymbol{F}|$ is represented in the rms value.

III. THEORETICAL BACKGROUND OF ELECTROABSORPTION SPECTROSCOPY

Energy levels of a molecule or molecular system are influenced by an electric field, depending on the magnitude of the permanent dipole moment $\boldsymbol{\mu}$ and the polarizability $\boldsymbol{\alpha}$ in the states under consideration. The field-induced change in the transition energy (ΔE) between ground (g) and excited (e) states is given by

$$\Delta E = -\Delta\boldsymbol{\mu}\cdot\boldsymbol{F} - \tfrac{1}{2}\boldsymbol{F}\cdot\Delta\boldsymbol{\alpha}\cdot\boldsymbol{F}, \tag{3}$$

where $\Delta\boldsymbol{\mu}$ and $\Delta\boldsymbol{\alpha}$ are the differences in the dipole moment and molecular polarizability tensor, respectively, between the ground and excited states, i.e., $\Delta\boldsymbol{\mu}=\boldsymbol{\mu}_e-\boldsymbol{\mu}_g$ and $\Delta\boldsymbol{\alpha}=\boldsymbol{\alpha}_e-\boldsymbol{\alpha}_g$. As a result, optical spectra show a shift or/and a broadening upon the application of the external electric fields.

By assuming an isotropic angular distribution of the molecules without the external electric field, the field-induced change in absorption intensity (ΔA) as a function of wavenumber ν can be expressed as the sum of the zeroth, first and second derivatives of the unperturbed absorption spectrum $A(\nu)$ as follows:[4,23]

$$\Delta A(\nu) = (fF)^2\left[A_\chi A(\nu) + B_\chi \nu\frac{d}{d\nu}\left\{\frac{A(\nu)}{\nu}\right\} + C_\chi \nu\frac{d^2}{d\nu^2}\left\{\frac{A(\nu)}{\nu}\right\}\right], \tag{4}$$

where f is the internal field factor and A_χ, B_χ, and C_χ are coefficients. On the assumption that the field-induced change in transition dipole moment is negligible, the coefficients A_χ, B_χ, and C_χ can be expressed as follows:

$$A_\chi = \frac{\mu_g^2}{30k^2T^2}(3\cos^2\chi-1)(3\cos^2\xi-1) + \frac{1}{10kT}(3\cos^2\chi-1)(\alpha_m-\bar{\alpha}), \tag{5}$$

$$B_\chi = \frac{\Delta\bar{\alpha}}{2hc} + \left\{\frac{(\Delta\alpha_m-\Delta\bar{\alpha})(3\cos^2\chi-1)}{10hc}\right\} + \frac{\mu_g\Delta\mu}{3hckT}\cos\gamma + \left(\frac{\mu_g\Delta\mu}{15hckT}\right)(3\cos^2\chi-1)(3\cos\eta\cos\xi-\cos\gamma), \tag{6}$$

$$C_\chi = (\Delta\mu)^2\left\{\frac{5+(3\cos^2\chi-1)(3\cos^2\eta-1)}{30h^2c^2}\right\}, \tag{7}$$

where c is the speed of light, k is Boltzmann constant, T is temperature, and μ_g is the magnitude of the ground state dipole moment, i.e., $|\boldsymbol{\mu}_g|$. $\Delta\alpha_m$ and α_m represent the diagonal component of $\Delta\boldsymbol{\alpha}$ and the polarizability in the ground state $\boldsymbol{\alpha}_g$ with respect to the direction of the transition moment, respectively. $\Delta\mu$ and $\Delta\bar{\alpha}$ are given by the following equations:

$$\Delta\mu = |\Delta\boldsymbol{\mu}| \quad \text{and} \quad \Delta\bar{\alpha} = \tfrac{1}{3}\mathrm{Tr}(\Delta\boldsymbol{\alpha}). \tag{8}$$

η is the angle between the direction of $\Delta\boldsymbol{\mu}$ and the transition dipole moment. ξ is the angle between $\boldsymbol{\mu}_g$ and the transition dipole moment, and γ is the angle between $\Delta\boldsymbol{\mu}$ and $\boldsymbol{\mu}_g$. Temperature-dependent terms in Eqs. (5) and (6) arise from the field-induced molecular reorientation. If molecules are completely immobile with a random orientation distribution, these terms can be neglected.

The zeroth derivative component A_χ [see Eq. (5)] arises from the deviation of the distribution of the ensemble of transition dipole moments from isotropy. The first term in Eq. (5) arises from the orientation of the ground state dipole moment, i.e., $\boldsymbol{\mu}_g$ along $\boldsymbol{F}$. The second term reflects an alignment along the $\boldsymbol{F}$ due to the polarizability anisotropy in the ground state. These reorientational effects along the field direction can be detected as a change in absorption intensity. Stark shift of the transition energy is not relevant to the zeroth derivative component.

The electronic response of a molecule to the applied field appears through the Stark shift of the transition energies [Eq. (3)]. If the polarizability change $\Delta\boldsymbol{\alpha}$ is significant, the Stark shift of the transition energy results in the redshift or blueshift of the absorption band. The first term in Eq. (6) is the isotropic component which does not depend on χ, and the second term is the χ-dependent component owing to the change in polarizability anisotropy on electronic transition. The resulting shape of the EA spectrum is the first derivative of the absorption spectrum. If the dipole moment change $\Delta\boldsymbol{\mu}$ following the light absorption is significant, the absorption band shape will broaden in the presence of $\boldsymbol{F}$, giving rise to the EA spectrum, the shape of which is the second derivative of the absorption spectrum.

The reorientation effect also contributes to the first derivative component. The third and fourth terms in Eq. (6) arise from the concerted effect of the orientation of $\boldsymbol{\mu}_g$ along the $\boldsymbol{F}$ and the linear Stark shift caused by the dipole moment change $\Delta\boldsymbol{\mu}$. This effect can be regarded as a manifestation of the field-induced orientation after the average over the Stark effect.

IV. RESULTS AND DISCUSSION

A. Electroabsorption spectra of C153

Polarized EA spectra of C153 in benzene solution were observed with a field strength of 0.1 MV cm^{-1}. The results are shown in Fig. 2, together with the absorption spectrum. The EA spectra remarkably depend on χ, i.e., on the angle between the field direction and the polarization direction of the absorption light, and the spectra could be simulated by a linear combination of the absorption and its derivative spectra, as expected from Eq. (4). The field-induced change in absorption intensity is proportional to the square of the strength of the applied electric field, as shown in Fig. 3. The simulated EA spectra as well as the observed spectra with $\chi=90°$ and 54.7° (magic angle) are shown in Figs. 4(a) and 4(b), respectively, together with absorption and its first derivative spectra in Fig. 4(c). The experimental values of the coefficients A_χ, B_χ, and C_χ used to simulate the observed EA spectra are listed in Table I. The zeroth derivative component, A_χ, is negligible at the magic angle of χ, as expected in Eq. (5). On the other hand, A_χ is negative with $\chi=90°$. By a change in χ from 54.7° to 90°, the field-induced change in

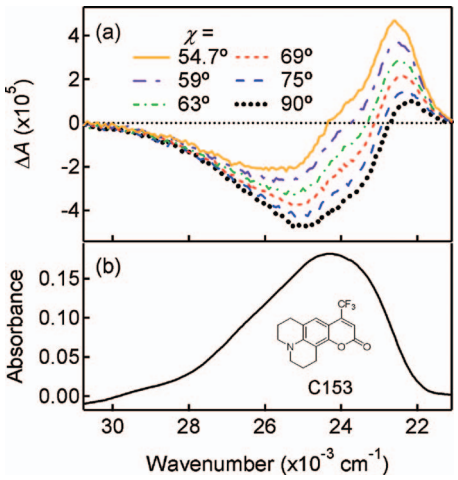

FIG. 2. (a) EA spectra of benzene solution of C153 observed with different angles of χ whose values are shown in the figure and (b) absorption spectrum of C153 in benzene observed with $\chi=90°$. Applied electric field was 0.10 MV cm^{-1}. Molecular structure of C153 is shown in the figure.

absorption intensity monotonically decreased [see Fig. 2(a)], suggesting that ξ, i.e., the angle between the dipole moment in the ground state ($\boldsymbol{\mu}_g$) and the transition moment is smaller than the magic angle [see Eq. (5)]. Actually, EA spectra observed at the magic angle of χ could be simulated by the first derivative of the absorption spectrum without consideration of the zeroth and second derivative components, as shown in Fig. 4. The magnitude of the second derivative component C_χ evaluated from the result in the polymer film is much smaller than the experimental error of the corresponding value in solution, as shown in Table I.

The transition moment polarizability and hyperpolarizability are considered to be negligible in C153,[19] and the zeroth derivative component in the EA spectrum can be ascribed to the field-induced reorientation of the C153 molecule. The first derivative component in the EA spectra arises from both electronic polarization and reorientational polarization. The former effect originates from the change in molecular polarizability ($\boldsymbol{\Delta\alpha}$) following absorption, while the latter effect originates from the field-induced reorientation of C153 molecules. In the EA spectra, the contribution of the first derivative in the EA spectra is much larger in solution than in PMMA, indicating that the first derivative component in solution mainly comes from the field-induced reorientation of C153 molecules; the first derivative component at the

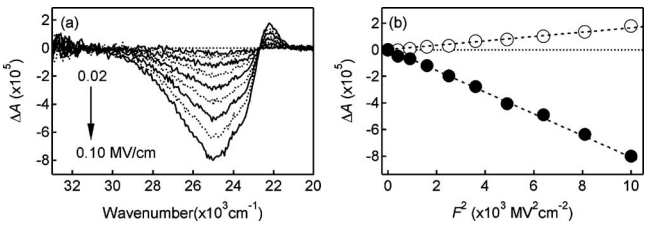

FIG. 3. (a) EA spectra of benzene solution of C153 observed with $\chi=90°$ at different field strengths from 0.02 to 0.10 MV cm^{-1} in every 0.01 MV cm^{-1} and (b) plots of the electric field-induced change in absorption intensity as a function of the square of the applied field strength monitored at 25 000 cm^{-1} (closed circle) and 22 200 cm^{-1} (open circle), respectively.

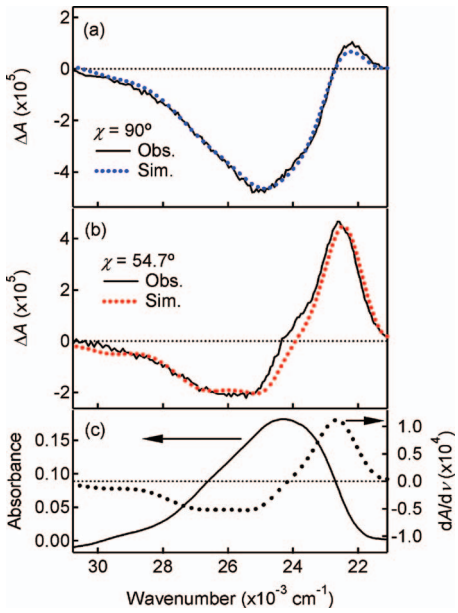

FIG. 4. (a) EA spectrum of benzene solution of C153 observed at 0.10 MV cm^{-1} with $\chi=90°$ (solid line) and the spectrum simulated by a linear combination between the zeroth and first derivatives of the absorption spectrum (dotted line), (b) EA spectrum of benzene solution of C153 observed at 0.10 MV cm^{-1} with $\chi=54.7°$ (solid line) and the first derivatives of the absorption spectrum (dotted line), and (c) absorption and its first derivative spectra of C153 in benzene.

magic angle of χ corresponds to the third term of right hand side of B_χ in Eq. (6), and the difference of the first derivative component between $\chi=54.7°$ and 90° comes from the fourth term of B_χ in Eq. (6). In fact, the contribution of the first derivative term estimated from the results in PMMA, which arises from the electronic polarization, is negligibly small, as shown in Table I. Then, $\mu_g\Delta\mu\cos\gamma$ and $(3\cos\eta\cos\xi-\cos\gamma)/\cos\gamma$ are determined by analyzing the first derivative component of the EA spectrum in benzene solution (see Table II). Based on the zeroth derivative component of the EA spectrum at $\chi=90°$, $\mu_g^2(3\cos^2\xi-1)$ is determined by assuming that the zeroth derivative component corresponds to the first term of Eq. (5), as shown in Table II. It is possible to rationalize this assumption by evaluating the second term in Eq. (5) from the magnitude of $f^2(\Delta\alpha_m-\Delta\bar{\alpha})$ determined by the data in the polymer film (see below). The contribution of the second term is expected to be smaller by one order of magnitude than that of the observed magnitude of the zeroth derivative component.

TABLE I. Coefficients used to simulate the EA spectra of C153. The experimental errors are shown in parenthesis.

Solvent or matrix	χ (deg)	A_χ (10^{-2} cm^2 MV^{-2})	B_χ (10 cm MV^{-2})	C_χ (10^4 MV^{-2})
Benzene	90	−2.3(±0.2)	1.8(±0.6)	0(±0.5)
	54.7	0	3.1(±0.3)	0(±0.7)
1,4-Dioxane	90	−2.7(±0.2)	2.4(±0.5)	0(±0.4)
	54.7	0	4.4(±0.4)	0(±0.7)
Chlorobenzene	90	−6.0(±0.6)	4.0(±0.8)	0(±1.5)
	54.7	0	7.2(±0.8)	0(±1.0)
PMMA	90	0	0.11	0.16
	54.7	0	0.17	0.24

TABLE II. EA results for C153 in different solvents.

Solvent	Benzene	1,4-Dioxane	Chlorobenzene
ε_S	2.28	2.21	5.71
$f^2\mu_g^2(3\cos^2\xi-1)$ (D^2)	108 (±12)	127 (±15)	281 (±30)
$f^2\mu_g\Delta\mu\cos\gamma$ (D^2)	65 (±7)	96 (±10)	157 (±17)
$(3\cos\eta\cos\xi-\cos\gamma)/\cos\gamma$	2.2 (±0.2)	2.2 (±0.2)	2.2 (±0.2)
$f\mu_g$[a] (D)	7.4 (±0.4)	8.1 (±0.5)	12.0 (±0.7)
$f\Delta\mu$[b] (D)	10.1 (±1.7)	13.6 (±2.4)	15.0 (±2.7)
$\Delta\mu$[c] (D)	7.0 (±1.1)	9.7 (±1.7)	5.8 (±1.0)
μ_g[c] (D)	5.2 (±0.3)	5.8 (±0.4)	4.7 (±0.3)
μ_e[c] (D)	11.9 (±1.5)	15.0 (±2.0)	10.2 (±1.2)

[a] $\xi=10°$ is used.
[b] $\gamma=29.5°$ is used.
[c] $f=(\varepsilon_S+2)/3$ is used.

EA spectra of C153 have been also obtained in 1,4-dioxane and monochlorobenzene. The results taken with $\chi=90°$ and 54.7° are shown in Fig. 5, together with the absorption and its derivative spectra. The EA spectra in both solutions, which depend on χ, are similar in shape to the ones in benzene solution. For example, the EA spectra of C153 in 1,4-dioxane or monochlorobenzene observed with $\chi=90°$ show a marked negative contribution of the zeroth derivative component, which originates from the field-induced reorientation effect, and the EA spectra could be simulated by a linear combination of the zeroth and first derivatives of the absorption spectrum. Based on the EA spectra in 1,4-dioxane and in monochlorobenzene, $\mu_g\Delta\mu\cos\gamma$, $(3\cos\eta\cos\xi-\cos\gamma)/\cos\gamma$, and $\mu_g^2(3\cos^2\xi-1)$ of C153 are also obtained, as shown in Table II.

In contrast with the EA spectra in solutions, the zeroth derivative component of C153 was negligibly small in PMMA irrespective of χ (see Fig. 6), suggesting that C153 molecules are immobilized in a PMMA film; the field-induced reorientation is negligible in PMMA even in the presence of electric field as strong as 0.7 MV cm^{-1}. In fact, the EA spectra of C153 in PMMA could be simulated by a linear combination of the first and second derivatives of the absorption spectrum.[19] From the EA spectra observed in PMMA at $\chi=54.7°$, where the first and second derivative components correspond to the first term of Eqs. (6) and (7), respectively, the magnitude of $f^2\Delta\bar{\alpha}$ and $f\Delta\mu$ have been determined to be 60 Å^3 and 7.2 D, respectively. With the internal field correction of $f=(\varepsilon_S+2)/3$, where ε_S is the dielectric constant, i.e., 3.6 in PMMA, the magnitudes of $\Delta\bar{\alpha}$ and $\Delta\mu$ are evaluated to be 17 Å^3 and 3.9 D, respectively. These values are roughly the same as the ones reported for C153 doped in the heated PMMA,[19] though the PMMA was not heated in the present experiments. Note that the former experiment was performed at 298 K,[19] which is almost identical to the temperature used in the present study. From the difference of the second derivative component of the EA spectra in PMMA between $\chi=90°$ and 54.7°, η, i.e., the angle between $\Delta\boldsymbol{\mu}$ and the transition dipole is determined to be 19.5°. Note that the second term of Eq. (7) is zero at $\chi=54.7°$, not zero at $\chi=90°$. By comparing the first derivative components of the EA spectra in PMMA between $\chi=90°$ and 54.7°, the value of $f^2(\Delta\alpha_m-\Delta\bar{\alpha})$ is determined to be 110 Å^3. Then, $f^2\Delta\alpha_m$ is estimated to be 170 Å^3 in PMMA.

Above-mentioned value of η, which was obtained to be 19.5° in PMMA, may be applicable to C153 in solution. By assuming that the dipole moments both in the ground state and in the excited states are located in the molecular plane, γ is determined to be 29.5° in every solution to reproduce the value of $(3\cos\eta\cos\xi-\cos\gamma)/\cos\gamma$ given in Table II. Then, ξ, i.e., the angle between $\boldsymbol{\mu}_g$ and the transition dipole moment is determined to be 10°. The magnitude of ξ was

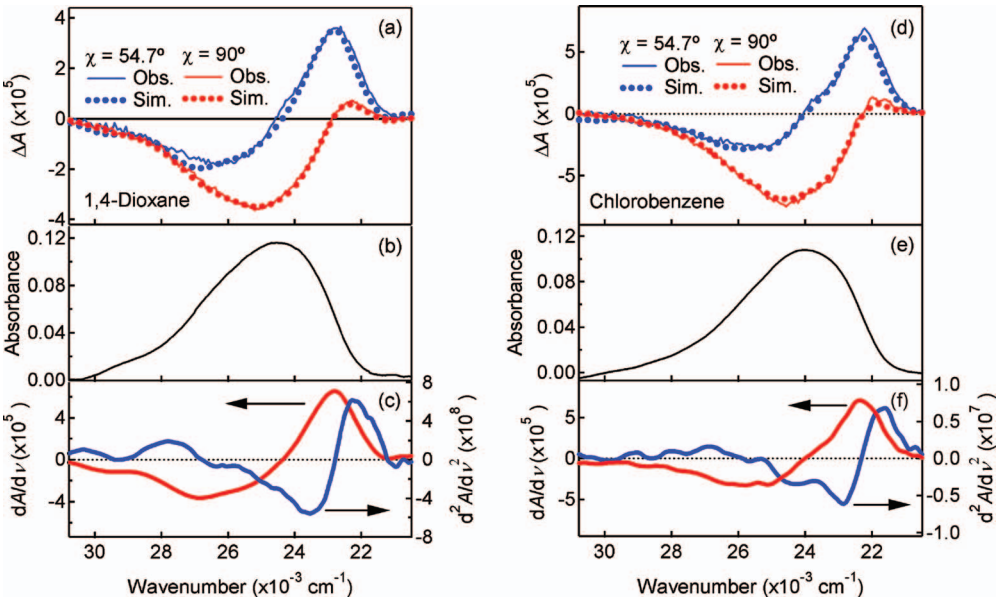

FIG. 5. EA spectra of C153 in 1,4-dioxane (left) and in monochlorobenzene (right) observed with a field strength of 0.10 MV cm^{-1}. [(a) and (d)] EA spectra observed with $\chi=90°$ (thin solid line) and $\chi=54.7°$ (thick solid line), respectively, and the simulated spectra (dotted line), [(b) and (e)] absorption spectrum of C153 observed with $\chi=90°$, and [(c) and (f)] the first and second derivatives of the absorption spectrum.

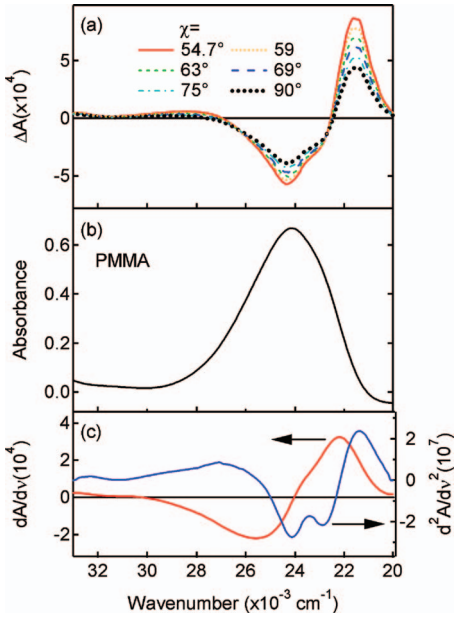

FIG. 6. (a) EA spectra of C153 in a PMMA film observed at 0.7 MV cm^{-1} with different angles of χ, whose values are shown in the figure, (b) absorption spectrum in PMMA, and (c) the first and second derivatives of the absorption spectrum.

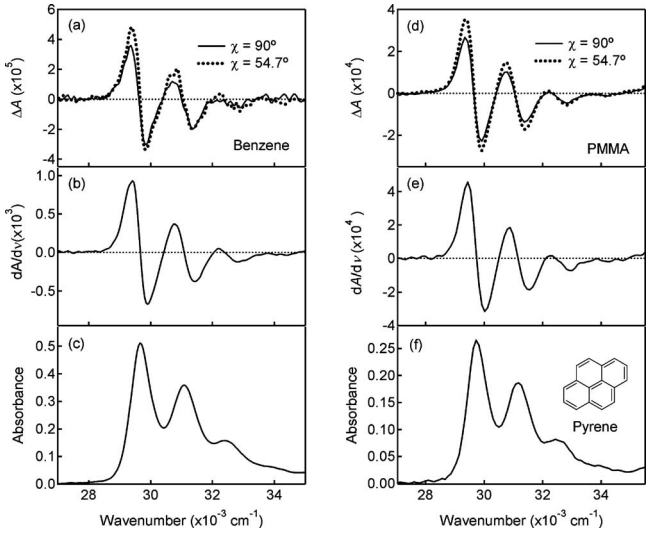

FIG. 7. Absorption and EA spectra of pyrene in benzene (left) and in PMMA (right). [(a) and (d)] EA spectra observed with $\chi=90°$ (solid line) and $\chi=54.7°$ (dotted line), [(b) and (e)] the first derivative of the absorption spectrum, and [(c) and (f)] absorption spectrum observed with $\chi=90°$. The applied field strength was 0.10 MV cm^{-1} in benzene and 1.0 MV cm^{-1} in PMMA. Molecular structure of pyrene is shown in the figure.

suggested to be as small as 3°–6°,[24] to which the present value is very similar. By employing these values of η, γ and ξ, $f\mu_g$ and $f\Delta\mu$ are evaluated.

The internal field factor f accounts for the enhancement in local field at the position of solute molecule in relation to the externally applied electric field.[25] By using the factor of $f=(\varepsilon_S+2)/3$, the dipole moment both in the ground state and in the excited state, i.e., μ_g and μ_e are obtained in each solvent, As shown in Table II, however, the magnitude of the dipole moment thus estimated is not constant, though both values of μ_g and μ_e are quite close to the ones determined in other experimental and theoretical methods.[19,24,26–34] Note that $\Delta\mu=7.1$ D evaluated in the gas phase[24] is also close to our results. To understand the solvent dependence of the present values of μ_g and μ_e, it may be necessary to consider the solute-solvent interaction in the molecular level and to perform further study. It should be also noticed that the magnitude of the change in dipole moment following absorption in any solution is much larger than that in PMMA.

B. Electroabsorption spectra of pyrene

Nonpolar molecules of pyrene doped in a PMMA film are regarded as immobilized even in the presence of electric fields, as reported previously,[20] and the EA spectra of pyrene in PMMA show the shape given by the first derivative of the absorption spectrum (see Fig. 7 and Table III). From the EA spectra with the magic angle of χ, the value of $f^2\Delta\bar{\alpha}$ was obtained to be 72 ± 10 Å^3 in PMMA, which is a little larger than the one obtained by assuming the isotropic molecular polarizability, i.e., $\Delta\bar{\alpha}=\Delta\alpha_m$. Note that 61 Å^3 was obtained in our pervious study by using nonpolarized light and $\chi=90°$.[20] With the internal field correction, we obtain $\Delta\bar{\alpha}=20\pm3$ Å^3. From the difference between the EA spectra obtained $\chi=54.7°$ and 90°, $f^2(\Delta\alpha_m-\Delta\bar{\alpha})$ is determined to be 24 ± 3 Å^3, i.e., $f^2\Delta\alpha_m$ is determined to be 96 ± 13 Å^3 in PMMA. With the internal field correction, we obtain $(\Delta\alpha_m-\Delta\bar{\alpha})=6.8\pm0.9$ Å^3 and $\Delta\alpha_m=27\pm3.7$ Å^3.

EA spectra of pyrene in benzene solution are also obtained for the S_2-S_0 transition with $\boldsymbol{F}=0.1$ MV cm^{-1}. The EA spectra obtained with $\chi=54.7°$ and 90° are shown in Fig. 7. The shape of the EA spectra is given by the first derivative of the absorption spectrum in both cases, as in the case of pyrene in PMMA, indicating that pyrene molecules are randomly distributed in benzene solution even in the presence of $\boldsymbol{F}$; pyrene molecules are not reoriented by application of the electric field because the electric dipole moment of pyrene in the ground state is zero and the orientational polarizability is negligible. Thus, the EA spectrum of pyrene results from the change in molecular polarizability following absorption not only in PMMA but also in solution. From the EA spectra observed with $\chi=54.7°$, $f^2\Delta\bar{\alpha}$ of pyrene in benzene is determined to be 130 ± 20 Å^3. By comparing the EA spectra observed in benzene at $\chi=54.7°$ and 90°, $f^2(\Delta\alpha_m-\Delta\bar{\alpha})$ is determined to be 80 ± 10 Å^3 for the S_2-S_0 absorption transition of pyrene. Then, $f^2\Delta\alpha_m$ is determined to be 210 ± 30 Å^3 in benzene. With the internal field correction, we obtain $\Delta\bar{\alpha}=63\pm9.8$ Å^3, $(\Delta\alpha_m-\Delta\bar{\alpha})=39\pm4.9$ Å^3, and $\Delta\alpha_m=103\pm14$ Å^3, respectively. The field-induced orientation is not necessary to be considered for pyrene both in a

TABLE III. Coefficients used to simulate the EA spectra of pyrene. The experimental errors are shown in parenthesis.

Solvent or matrix	χ (deg)	A_χ (cm^2 MV^{-2})	B_χ (cm MV^{-2})	C_χ (MV^{-2})
Benzene	90	0	3.2(±0.6)	0
	54.7	0	3.6(±0.6)	0
PMMA	90	0	1.8(±0.3)	0
	54.7	0	2.0(±0.3)	0

polymer film and in solution, in contrast with C153, in which orientational polarizability plays a significant role in the EA spectra in solution. It is worth mentioning that $\Delta\bar{\alpha}$ as well as $\Delta\alpha_m$ of pyrene in benzene is larger than that in PMMA after a simple Lorentz field correction by adopting the f, though the reason is not known well.

V. SUMMARY

We developed a liquid cell for the EA measurements of solution samples, and polarized EA spectra in solutions and in polymer films were measured and compared to each other. For a polar molecule of C153 in solutions, the marked χ dependence of the shape of the EA spectra was observed; the zeroth derivative component of the absorption spectrum is not negligible in the EA spectra of C153 in solution except for $\chi=54.7°$, which comes from the χ dependence of the field-induced change in absorption intensity. The presence of the zeroth derivative component demonstrates that the C153 molecules are reorientated in solutions by application of electric field. In contrast with C153 in solutions, the zeroth derivative component was negligible in the EA spectra of C153 doped in a PMMA film, indicating that C153 molecules are immobilized in PMMA even in the presence of electric fields. Nonpolar molecules of pyrene show the EA spectra which are similar in shape to the first derivative of the absorption spectrum both in solution and in PMMA, and the zeroth derivative component of the absorption spectrum is negligible, indicating that the molecular reorientation of pyrene caused by the applied electric field is negligible both in solutions and in PMMA. Based on the analysis of the EA spectra, the magnitude of the electric dipole moment both in the ground state and in the excited state were evaluated for C153. The magnitudes of the polarizability and its anisotropy of pyrene were evaluated both in PMMA and in benzene solution, and it is shown that the magnitude of the change in polarizability in benzene is much larger than in PMMA.

ACKNOWLEDGMENTS

We thank Professor M. Yamamoto and Dr. K. Matsuda (Division of Electronics for Informatics, Hokkaido University) for helping the evaporation of silicon oxide thin films on the substrates. We also thank Mr. T. Okada for his help in the measurements of the EA spectra of pyrene.

[1] B. Friedrich and D. R. Herschbach, Nature (London) **353**, 412 (1991).
[2] H. Loesch, J. Phys. Chem. A **101**, 7461 (1997) (special issue on Stereodynamics of Chemical Reaction).
[3] J. Michl and E. W. Thulstrup, *Spectroscopy with Polarized Light Solute Alignment by Photoselection, in Liquid Crystals, Polymers, and Membranes* (Wiley, New York, 1986).
[4] W. Liptay, in *Excited States*, edited by E. C. Lim (Academic, New York, 1974), Vol. 1, p. 129.
[5] R. M. Hochstrasser, Acc. Chem. Res. **6**, 263 (1973).
[6] R. Mathies and A. C. Albrecht, J. Chem. Phys. **60**, 1420 (1974).
[7] G. U. Bublitz and S. G. Boxer, Annu. Rev. Phys. Chem. **48**, 213 (1997).
[8] S. A. Locknar and L. A. Peteanu, J. Phys. Chem. B **102**, 4240 (1998).
[9] F. W. Vance, R. D. Williams, and J. T. Hupp, Int. Rev. Phys. Chem. **17**, 307 (1998).
[10] N. Ohta, Bull. Chem. Soc. Jpn. **75**, 1637 (2002).
[11] M. S. Mehata, T. Iimori, T. Yoshizawa, and N. Ohta, J. Phys. Chem. A **110**, 10985 (2006).
[12] E. Jalviste and N. Ohta, J. Chem. Phys. **121**, 4730 (2004).
[13] R. Mathies and L. Stryer, Proc. Natl. Acad. Sci. U.S.A. **73**, 2169 (1976).
[14] H. Hiramatsu and H. Hamaguchi, Appl. Spectrosc. **58**, 355 (2004).
[15] A. Kocot, J. K. Vij, and T. S. Perova, Adv. Chem. Phys. **113**, 203 (2000).
[16] R. Kanya and Y. Ohshima, Phys. Rev. A **70**, 013403 (2004).
[17] E. Lippert, Z. Naturforsch. B **10a**, 541 (1955).
[18] N. Mataga, Y. Kaifu, and M. Koizumi, Bull. Chem. Soc. Jpn. **28**, 69 (1955).
[19] A. Chowdhury, S. A. Locknar, L. L. Premvardhan, and L. A. Peteanu, J. Phys. Chem. A **103**, 9614 (1999).
[20] S. Umeuchi, Y. Nishimura, I. Yamazaki, H. Murakami, M. Yamashita, and N. Ohta, Thin Solid Films **311**, 239 (1997).
[21] T. Iimori, A. M. Ara, T. Yoshizawa, T. Nakabayashi, and N. Ohta, Chem. Phys. Lett. **402**, 206 (2005).
[22] *Handbook of Chemistry and Physics*, edited by R. C. Weast (CRC, Boca Raton, 1980).
[23] E. Jalviste and N. Ohta, J. Photochem. Photobiol. C **8**, 30 (2007).
[24] R. Kanya and Y. Ohshima, Chem. Phys. Lett. **370**, 211 (2003).
[25] C. J. F. Bottcher and P. Bordewijk, *Theory of Electric Polarization* (Elsevier, Amsterdam, 1978), Vol. 1.
[26] P. K. McCarthy and G. J. Blanchard, J. Phys. Chem. **97**, 12205 (1993).
[27] F. Cichos, R. Brown, and Ph. A. Bopp, J. Chem. Phys. **114**, 6834 (2001).
[28] P. V. Kumar and M. Maroncelli, J. Chem. Phys. **103**, 3038 (1995).
[29] D. V. Matyushov and M. D. Newton, J. Phys. Chem. A **105**, 8516 (2001).
[30] A. Mühlpfordt, R. Schanz, N. P. Ernsting, V. Farztdinov, and S. Grimme, Phys. Chem. Chem. Phys. **1**, 3209 (1999).
[31] K. Rechthaler and G. Kohler, Chem. Phys. **189**, 99 (1994).
[32] W. Baumann and Z. Nagy, Pure Appl. Chem. **65**, 1729 (1993).
[33] S. N. Smirnov and C. L. Braun, Rev. Sci. Instrum. **69**, 2875 (1998).
[34] A. Samanta and R. W. Fessenden, J. Phys. Chem. A **104**, 8577 (2000).